

NO PARAMETERS LEFT BEHIND: SENSITIVITY GUIDED ADAPTIVE LEARNING RATE FOR TRAINING LARGE TRANSFORMER MODELS

Chen Liang*, Haoming Jiang[†], Simiao Zuo*, Pengcheng He*, Xiaodong Liu[◊],
 Jianfeng Gao[◊], Weizhu Chen* & Tuo Zhao*

* Georgia Institute of Technology, [†] Amazon, [◊] Microsoft Azure AI, [◊] Microsoft Research
 {cliang73, simiaozuo, tourzhao}@gatech.edu
 jhaoming@amazon.com
 {penhe, xiaodl, jfgao, wzchen}@microsoft.com

ABSTRACT

Recent research has shown the existence of significant redundancy in large Transformer models. One can prune the redundant parameters without significantly sacrificing the generalization performance. However, we question whether the redundant parameters could have contributed more if they were properly trained. To answer this question, we propose a novel training strategy that encourages all parameters to be trained sufficiently. Specifically, we adaptively adjust the learning rate for each parameter according to its sensitivity, a robust gradient-based measure reflecting this parameter’s contribution to the model performance. A parameter with low sensitivity is redundant, and we improve its fitting by increasing its learning rate. In contrast, a parameter with high sensitivity is well-trained, and we regularize it by decreasing its learning rate to prevent further overfitting. We conduct extensive experiments on natural language understanding, neural machine translation, and image classification to demonstrate the effectiveness of the proposed schedule. Analysis shows that the proposed schedule indeed reduces the redundancy and improves generalization performance.

1 INTRODUCTION

Large-scale Transformer models have achieved remarkable success in various fields. Performance of these models scales with their number of parameters, which can be up to hundreds of millions, e.g., BERT (Devlin et al., 2018), DeBERTa (He et al., 2020), GPT-3 (Brown et al., 2020). Recent research, however, has shown the existence of significant redundancy in the Transformer models (Michel et al., 2019; Fan et al., 2019; Wang et al., 2019; Chen et al., 2020; Sanh et al., 2020). For example, Sanh et al. (2020) removes around 90% of the parameters, and the models exhibit only a marginal performance drop.

The existence of redundancy can hurt the model performance. Recent works have demonstrated that the removal of the redundant parameters can lead to better generalization performance, a phenomenon observed in both small-scale models (Mozer & Smolensky, 1989; Rasmussen & Ghahramani, 2001; Grünwald & Grunwald, 2007) and large-scale Transformer models (Bartoldson et al., 2019; Voita et al., 2019; Hou et al., 2020; Liang et al., 2021). As illustrated in Figure 1, with up to 20% of the parameters pruned, the generalization performance boosts up to 1%.

As a result, we aim to improve model generalization through redundancy elimination. However, the existence of redundancy has long been regarded as inevitable. The common belief is that, in each network, there always exists a set of parameters “born” to be useless (Frankle & Carbin, 2018; Liu et al., 2018). Following this belief, pruning, where redundant parameters are directly zeroed out,

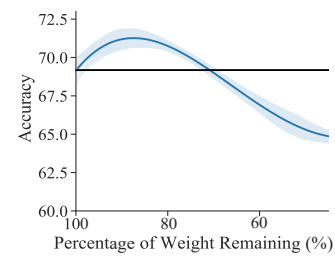


Figure 1: Validation results of fine-tuning BERT-base at different sparsity levels on the RTE dataset (Wang et al., 2018) in Liang et al. (2021). Solid black curve represents the full model performance.

becomes one of the most widely adopted solutions to redundancy elimination. However, we ask a critical question here:

Are these parameters really redundant, or just insufficiently trained by commonly used training strategies?

Our question is motivated by empirical observations, which show that training strategies indeed play a role in causing redundancy. For example, different learning rates (Table 1), random seeds and optimizers (Morcos et al., 2019) can produce models with similar performance but different sets of redundant parameters. This suggests that the redundancy of parameters depends on the training strategy: A training strategy often prefers specific parameters and provides them with sufficient training. In contrast, the other parameters receive insufficient training and become under-fitted. As a result, these parameters become redundant, such that they fail to contribute to the generalization and prevent the model from achieving its ideal performance. Therefore, we hypothesize that with a desirable training strategy, these redundant parameters can receive more sufficient training and become useful ultimately.

We verify the hypothesis by proposing a novel training strategy, which encourages all parameters to be trained sufficiently. Throughout the training process, we simultaneously excite the under-fitted parameters to reduce redundancy and regularize the well-fitted parameters to prevent overfitting.

More specifically, we propose an adaptive learning rate schedule – SAGE (Sensitivity-guided Adaptive learninG ratE), where each parameter learns at its own pace guided by its sensitivity. Sensitivity originated in model pruning, where it is used to measure the redundancy of the parameters (Molchanov et al., 2016; 2019; Theis et al., 2018; Lee et al., 2018; Ding et al., 2019). In pruning literature, parameters with low sensitivity are considered redundant. Since a redundant parameter could be insufficiently trained and under-fitted, we promote its training by increasing its learning rate. In contrast, for a parameter with high sensitivity, i.e., it is considered sufficiently trained and well-fitted, we slow down its training by decreasing its learning rate to prevent overfitting.

Moreover, we introduce a local temporal variation of the sensitivity as a second factor to further guide the learning rate. The local temporal variation essentially measures the uncertainty of sensitivity, which mainly comes from two sources: (1) The sensitivity can have large variance due to data sampling. This is because during training, the sensitivity is evaluated using a randomly sampled mini-batch instead of all the training data. (2) The sensitivity of a parameter may not be stable and can vary drastically among iterations, which introduces extra uncertainty. We define the local temporal variation of a parameter as the absolute difference between its sensitivity and an exponential moving average of its sensitivity from all previous iterations. A large local temporal variation implies high uncertainty in the sensitivity at the current iteration, and therefore it is not yet a reliable indicator of redundancy. Accordingly, we should avoid significantly decreasing its learning rate even though its sensitivity at the current iteration might be large.

Therefore, we eventually require the overall learning rate schedule for each parameter to be proportional to the ratio between the local temporal variation and the sensitivity. This can effectively account for the uncertainty issue in sensitivity.

We conduct experiments on a wide range of tasks and models to demonstrate the effectiveness of SAGE. In natural language understanding, the fine-tuning performance of BERT-base (Devlin et al., 2018) and RoBERTa-large (Liu et al., 2019b) improves 1.4 and 0.6 task-average score on the dev set of the GLUE benchmark (Wang et al., 2018), respectively. Furthermore, SAGE improves neural machine translation performance using Transformer-base (Vaswani et al., 2017) on two datasets, suggesting it also benefits training-from-scratch. SAGE also boost the image classification accuracy on ImageNet dataset (Deng et al., 2009) with Vision Transformer models (Dosovitskiy et al., 2020). Furthermore, our experiments demonstrate SAGE is complementary to various types of optimizers, e.g., SGD (Robbins & Monro, 1951), Adam, and Adamax (Kingma & Ba, 2014).

OVLP Among	Avg % OVLP
2 Models	59.8%
3 Models	46.5%
5 Models	35.7%

Table 1: Percentage of overlapping between the 30% most redundant parameters in 5 BERT-base models fine-tuned using $\{1, 5, 8, 10, 20\} \times 10^{-5}$ as learning rates on SST-2.

Moreover, we observe several favorable proprieties of SAGE. First, it leads to balanced and sufficient training on all parameters and produces a better-generalized model. Second, SAGE is complementary to state-of-the-art training methods. Specifically, we show that SAGE achieves better performance on GLUE when combined with adversarial regularization (Jiang et al., 2019). Our code has been released at <https://github.com/ciliang1453/SAGE>.

2 PRELIMINARY

We briefly review the sensitivity of the parameters and adaptive learning rate methods.

2.1 SENSITIVITY OF THE PARAMETERS

The sensitivity of a parameter essentially approximates the change in the loss magnitude when this parameter is completely zeroed-out (LeCun et al., 1990; Mozer & Smolensky, 1989). If the removal of a parameter causes a large influence on the loss, then the model is sensitive to it. More specifically, we define a deep neural network with parameters $\Theta = [\theta_1, \dots, \theta_J] \in \mathbb{R}^J$, where for $j = 1, \dots, J$, $\theta_j \in \mathbb{R}$ denotes each parameter. We further define $\Theta_{j,-j} = [0, \dots, 0, \theta_j, 0, \dots, 0] \in \mathbb{R}^J$. We denote the loss of the model as $L(\Theta)$, and the gradients of the loss with respect to Θ as $\nabla_\Theta L(\Theta)$. The sensitivity of the j -th parameter is defined as the magnitude of the gradient-weight product:

$$I_j = |\Theta_{j,-j}^\top \nabla_\Theta L(\Theta)|. \quad (1)$$

This definition is derived from the first-order Taylor expansion of $L(\cdot)$ with respect to θ_j at Θ . Specifically, I_j approximates the absolute change of the loss given the removal of θ_j :

$$\Theta_{j,-j}^\top \nabla_\Theta L(\Theta) \approx L(\Theta) - L(\Theta - \Theta_{j,-j}).$$

The sensitivity was originally introduced for model pruning (Molchanov et al., 2016; 2019; Theis et al., 2018; Lee et al., 2018; Ding et al., 2019; Xiao et al., 2019), and it was commonly used as an ‘importance score’ for model weights. The parameters with high sensitivity are of high importance and should be kept (Lubana & Dick, 2020). Parameters with low sensitivity are considered redundant, and they can be safely pruned with only marginal influence on the model loss.

2.2 ADAPTIVE LEARNING RATE METHODS

Adaptive learning rate methods adjust the learning rate of each individual parameter based on the training progress. Most of these methods focus on adapting the training to the optimization landscape, e.g., AdaGrad (Duchi et al., 2011), AdaDelta (Zeiler, 2012), RMSProp (Hinton et al., 2012), Adam (Kingma & Ba, 2014) and RAdam (Liu et al., 2019a). Their purpose is to make the model converge faster to the first-order stationary solutions. Specifically, these methods prefer updating the weights with smaller second-order moments, as the loss function is generally flat along directions corresponding to such weights.

There are also some adaptive learning rate methods focusing on the perspective of improving model generalization (Loshchilov & Hutter, 2018; Foret et al., 2020). For example, AdamW (Loshchilov & Hutter, 2018) propose to decouple the weight decay and gradient update to avoid regularizing weights that have larger gradient magnitudes with a weaker strength.

3 METHOD

We introduce our proposed adaptive learning rate schedule, SAGE. Our method customizes a specific learning rate for each parameter at each iteration. A parameter’s learning rate at a certain iteration is determined by two factors: sensitivity and its local temporal variation.

Sensitivity of the parameters. At the t -th iteration, following Eq. (1), we define the sensitivity of $\theta_j^{(t)}$ as

$$I_j^{(t)} = |\Theta_{j,-j}^{(t)\top} \nabla_{\Theta^{(t)}} L(\Theta^{(t)})|, \quad (2)$$

which reflects the influence of removing $\theta_j^{(t)}$ in the model loss. In previous literature, $\theta_j^{(t)}$ is considered redundant when $I_j^{(t)}$ is small. In contrast, we hypothesize that $\theta_j^{(t)}$ is just insufficiently trained and under-fitted, and can become less redundant when receiving further training.

Local temporal variation. Recall that the sensitivity measure involves excessive uncertainty, which comes from: (1) Sensitivity is measured based on a randomly sampled mini-batch of the training data

at each iteration, which leads to a large variance; (2) Sensitivity can be unstable and vary drastically, as changes of the model introduce extra uncertainty to the measure.

One way to measure the uncertainty of sensitivity of θ_j is the absolute change of sensitivity, i.e., $|I_j^{(t)} - I_j^{(t-1)}|$. Such a quantity often has a large variance in practice. Therefore, we propose to keep track of an exponential moving average of $I_j^{(t)}$ as

$$\widehat{I}_j^{(t)} = \beta_0 \widehat{I}_j^{(t-1)} + (1 - \beta_0) I_j^{(t)},$$

where $\widehat{I}_j^{(0)} = 0$ and $\beta_0 \in (0, 1)$ is a hyper-parameter. Based on $\widehat{I}_j^{(t)}$, we measure the uncertainty of the j -th parameter's sensitivity using the local temporal variation defined as:

$$U_j^{(t)} = |I_j^{(t)} - \widehat{I}_j^{(t)}|. \quad (3)$$

We remark that a large $U_j^{(t)}$ implies that there exists high uncertainty in $I_j^{(t)}$, and therefore it is not yet a reliable indicator of the redundancy of $\theta_j^{(t)}$.

Algorithm. We denote the learning rate at the t -th iteration as $\eta^{(t)}$ under the original schedule. Then the sensitivity-guided learning rate for the j -th parameter at the t -th iteration can be computed as

$$\eta_j^{(t)} = \eta^{(t)} \cdot \frac{U_j^{(t)} + \epsilon}{\widehat{I}_j^{(t)} + \epsilon} = \eta^{(t)} \cdot \frac{|I_j^{(t)} - \widehat{I}_j^{(t)}| + \epsilon}{\widehat{I}_j^{(t)} + \epsilon}, \quad (4)$$

where $0 < \epsilon \ll 1$ prevents zero learning rate and zero denominator. Algorithm 2 shows the SAGE algorithm for SGD, and extensions to other algorithms, such as Adam (Kingma & Ba, 2014), are straightforward (Appendix A.4.1).

In Eq. (4), we place $\widehat{I}_j^{(t)}$ in the denominator, as one of our goals is to encourage all parameters to be sufficiently trained. If $\widehat{I}_j^{(t)}$ is small, we promote its training by increasing its learning rate. If $\widehat{I}_j^{(t)}$ is large, we slow down its training to prevent overfitting by decreasing its learning rate.

We place $U_j^{(t)}$ in the numerator to measure the uncertainty in the sensitivity. A large $U_j^{(t)}$ implies $I_j^{(t)}$ is not yet a reliable indicator of the redundancy in $\theta_j^{(t)}$. We thus avoid significantly decreasing its learning rate.

Algorithm 1 SGD-SAGE (\odot denotes Hadamard product and \oslash denotes Hadamard division)

Input: Model parameters $\Theta \in \mathbb{R}^J$; Data \mathcal{D} ; Learning rate schedule $\eta(\cdot)$; Total training iteration T ; Moving average coefficient β_0 .

- 1: Initialize $\widehat{I}^{(0)} = \mathbf{0} \in \mathbb{R}^J$.
- 2: **for** $t = 1, \dots, T$ **do**
- 3: Sample a minibatch $b^{(t)}$ from \mathcal{D} .
- 4: Compute gradient $\nabla_{\Theta^{(t)}} L(b^{(t)}, \Theta^{(t)})$.
- 5: $I^{(t)} = |\Theta^{(t)} \odot \nabla_{\Theta^{(t)}} L(b^{(t)}, \Theta^{(t)})|$.
- 6: $\widehat{I}^{(t)} = \beta_0 \widehat{I}^{(t-1)} + (1 - \beta_0) I^{(t)}$.
- 7: $U^{(t)} = |I^{(t)} - \widehat{I}^{(t)}|$.
- 8: $\Theta^{(t+1)} = \Theta^{(t)} - \eta^{(t)} (U^{(t)} + \epsilon) \oslash (\widehat{I}^{(t)} + \epsilon) \odot \nabla_{\Theta^{(t)}} L(b^{(t)}, \Theta^{(t)})$.
- 9: **end for**

Computation and memory usage. SAGE adds a marginal cost to computation and memory usage. At each iteration, we only perform an extra element-wise multiplication between the weight matrix and the corresponding gradient matrix obtained through back-propagation. The only memory cost is to store the exponential moving average of sensitivity.

4 EXPERIMENTS

We evaluate SAGE on widely used benchmarks for natural language understanding (NLU), neural machine translation (NMT), and image classification.

4.1 NATURAL LANGUAGE UNDERSTANDING

Model and data. We evaluate the fine-tuning performance of the pre-trained language models, BERT-base (Devlin et al., 2018) and RoBERTa-large (Liu et al., 2019b), on the General Language Understanding Evaluation (GLUE, Wang et al. (2018)) benchmark. GLUE contains nine NLU tasks, including textual entailment, question answering, sentiment analysis, and text similarity. Details about the benchmark are deferred to Appendix A.1.1.

Implementation Details. We implement our method using the MT-DNN code-base¹. We follow the suggested training and hyper-parameters settings from Liu et al. (2020). Specifically, we adopt Adam and Adamax (Kingma & Ba, 2014) with corrected weight decay (Loshchilov & Hutter, 2018) as the baseline optimizer and we set $\beta = (0.9, 0.999)$. We use a linear-decay learning rate schedule, and we apply SAGE to both Adam and Adamax.

We select learning rates in range of $\{1, 2, 3, 5, 8\} \times \{10^{-5}, 10^{-4}\}$. We select β_0 in range of $[0.6, 0.9]$ with an increment of 0.05. Other training details are reported in Appendix A.1.2.

Main results. Table 2 and Table 3 show the evaluation results on the GLUE benchmark. The dev results are averaged over 5 different random seeds, and all gains are statistically significant². We select the best single task model for test evaluation.

Model	Optimizer	RTE	MRPC	CoLA	SST-2	STS-B	QNLI	QQP	MNLI-m/mm	Average
		Acc	Acc/F1	Mcc	Acc	P/S Corr	Acc	Acc/F1	Acc	Score
BERT _{BASE}	Devlin et al. (2018)	-	-/86.7	-	92.7	-/-	88.4	-/-	84.4/-	-
	Adam	63.5	84.1/89.0	54.7	92.9	89.2/88.8	91.1	90.9/88.1	84.5/84.4	81.5
	Adam-SAGE	73.3	87.0/90.9	60.3	93.5	90.3/89.9	91.7	91.2/88.1	84.7/84.8	84.0
	Adamax	69.2	86.2/90.4	57.8	92.9	89.7/89.2	91.2	90.9/88.0	84.5/84.4	82.8
RoBERTa _{LARGE}	Adamax-SAGE	74.0	87.3/91.0	59.7	93.8	90.3/89.8	91.8	91.2/88.2	85.0/85.2	84.2
	Liu et al. (2019b)	86.6	-/90.9	68.0	96.4	92.4/-	94.7	92.2/-	90.2/90.2	-
	Adamax	86.6	90.4/93.1	67.5	96.4	92.4/92.2	94.7	92.1/89.3	90.4/90.3	88.7
	Adamax-SAGE	87.8	91.5/93.9	68.7	96.7	92.7/92.4	94.9	92.2/89.4	90.8/90.4	89.3

Table 2: Single task fine-tuning dev results on GLUE. All results are from our implementations. ‘-’ denotes missing results.

Our method gains 1.4 on dev and 1.1 on test of the task-average score on BERT-base. In large datasets, i.e., MNLI (392K) and QNLI (108K), SAGE improves around 0.5 points. In small datasets, i.e., RTE (2.5K) and CoLA (8.5K), we obtain more than 2 points of improvements. Such observations indicate that SAGE is very effective on the small datasets. Furthermore, SAGE improves upon RoBERTa-large by 0.6 average scores, suggesting SAGE can still achieve significant improvements for larger and more adequately pre-trained models than BERT-base.

	RTE	MRPC	CoLA	SST-2	STS-B	QNLI	QQP	MNLI-m/mm	Average
	Acc	F1	Mcc	Acc	P/S Corr	Acc	F1	Acc	Score
BERT _{BASE} (Devlin et al., 2018)	66.4	88.9	52.1	93.5	85.8	90.5	71.2	84.6/83.4	79.6
BERT _{BASE} , Adamax	66.8	88.6	54.0	93.4	86.6	90.6	71.1	84.7/83.6	79.9
BERT _{BASE} , Adamax-SAGE	69.8	89.7	54.5	94.1	87.1	90.8	71.3	84.9/83.8	80.7

Table 3: Single task fine-tuning test results from the GLUE evaluation server.

Model	Optimizer	IWSLT’14 De-En		WMT’16 En-De	
		34.5	27.3	35.1	27.7
Transformer _{BASE}	Adam				
Transformer _{BASE}	Adam-SAGE				

Table 4: Neural machine translation BLEU scores on test set. All results are from our implementation.

¹<https://github.com/namisan/mt-dnn>

²The dev results on RoBERTa-large are averaged over 3 different random seeds. All results have passed a paired student t-test with p-values less than 0.05. The detailed statistics are summarized in Appendix A.1.3.

Model	Optimizer	CIFAR100	ImageNet
ViT-B/32	SGD*	91.97	81.28
	SGD-SAGE	92.68	81.72
ViT-L/32	SGD*	93.04	80.99
	SGD-SAGE	93.74	81.90

Table 5: Image classification test accuracy. Results with * are from Dosovitskiy et al. (2020). ViT-B/32 and ViT-L/32 each denotes ViT-base and ViT-large model with 32×32 input patch size.

4.2 NEURAL MACHINE TRANSLATION

Model and Data. We evaluate SAGE on the Transformer-base NMT models (Vaswani et al., 2017) using two widely used NMT datasets, IWSLT’14 De-En (Cettolo et al., 2015)³ and WMT’16 En-De (Bojar et al., 2016)⁴. IWSLT’14 De-En is a low-resource dataset, which contains 160K sentence pairs. WMT’16 En-De is a rich-resource dataset, which contains 4.5M sentence pairs. Dataset and pre-processing details are deferred to Appendix A.2.1.

Implementation Details. We implement the algorithms using the *fairseq* code-base and follow the training and hyper-parameters settings from Ott et al. (2018; 2019). Specifically, we adopt the inverse square root learning rate schedule and we employ Adam (Kingma & Ba, 2014) as the optimizer with $\beta = (0.9, 0.98)$. We apply SAGE to the same setting.

We select learning rates in range of $\{5, 7\} \times 10^{-5} \cup \{1, 2\} \times 10^{-4}$ and select β_0 in range of $\{0.5, 0.6, 0.7, 0.8, 0.9\}$. Comprehensive training details are reported in Appendix A.2.2.

Main results. Table 4 shows the BLEU scores on the IWSLT’14 De-En and the WMT’16 En-De test set, where SAGE improves around 0.6 and 0.4 points, respectively. This suggests that other than fine-tuning, SAGE can also improve the generalization of trained-from-scratch models in both low-resource and rich-resource settings.

4.3 IMAGE CLASSIFICATION

Model and data. We evaluate SAGE using Vision Transformer models (ViT) on the CIFAR100 (Krizhevsky et al., 2009) and ILSVRC-2012 ImageNet dataset (Deng et al., 2009). Specifically, we evaluate the fine-tuning performance of the ViT-base and ViT-large pre-trained using ImageNet-21k, a superset of ImageNet dataset with 21k classes and 14M images. Data and pre-processing details are deferred to Appendix A.3.1.

Implementation details. All experiments follow the suggested training configuration of Dosovitskiy et al. (2020) and a jax-implemented code base⁵. We adopt SGD as the baseline optimizer with a momentum factor 0.9. We fine-tune the models for 100K steps for CIFAR100, and 200K steps for ImageNet. We select learning rates in range of $\{0.02, 0.05, 0.08, 0.1\}$ and select β_0 in range of $\{0.85, 0.90, 0.95\}$. Comprehensive training details are reported in Appendix A.3.2.

Main results. Table 5 shows the evaluation results on CIFAR100 and ImageNet. SAGE outperforms baselines by a significant margin. This demonstrates that SAGE is quite general, and can be applied to various tasks (e.g., NLP and computer vision) and optimizers (e.g., Adam, Adamax and SGD).

5 ANALYSIS

We verify that SAGE leads to more sufficient training (Section 5.1), better generalization performance (Section 5.2), and is complementary to existing state-of-the-art regularization methods (Section 5.3). We also provide ablation studies in Appendix A.4.4.

5.1 SAGE LEADS TO MORE SUFFICIENT TRAINING

Recall that SAGE adjusts the learning rate for each parameter according to two factors: the sensitivity of parameters and the local temporal variation of sensitivity. By inspecting these factors, we verify that SAGE leads to more sufficient training.

³<https://wit3.fbk.eu/>

⁴<http://data.statmt.org/wmt16/translation-task/>

⁵https://github.com/google-research/vision_transformer

The sensitivity distribution is more concentrated. Figure 2 shows the sensitivity distribution of parameters in the SAGE optimized models and the baseline models. We select the hyper-parameters that yield the best generalization performance on the BERT-base model, and we evaluate the sensitivity of each parameter using the entire training set. See Appendix A.4.2 for implementation details.

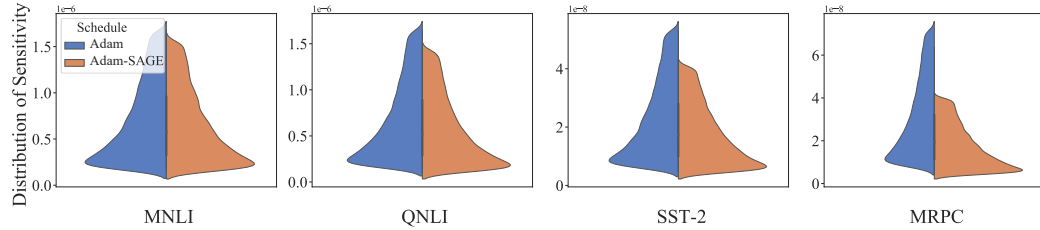


Figure 2: The sensitivity distribution of the BERT-base models fine-tuned on GLUE tasks. Note that we drop some outliers to ease visualization.

We observe that the sensitivity distribution exhibits a lower variance in the SAGE optimized models than the baseline models. This suggests that the sensitivity of parameters becomes more concentrated. In other words, the amount of each parameter’s contribution is more balanced, and the model is more sufficiently trained.

Even the most redundant parameters contribute to the model performance. Recall that sensitivity is a type of importance score in pruning, which is a straightforward approach to measure each parameter’s contribution. Therefore, we conduct an unstructured, one-shot pruning experiment on the fine-tuned BERT-base models. Specifically, we remove up to 40% parameters⁶ with the lowest sensitivity scores and evaluate the pruned models’ performance. We average the results over 5 models trained with different random seeds. Figure 3 *Upper* shows the generalization performance of the pruned models. To ease the comparison, Figure 3 *Lower* shows the change in generalization performance with respect to the un-pruned models.

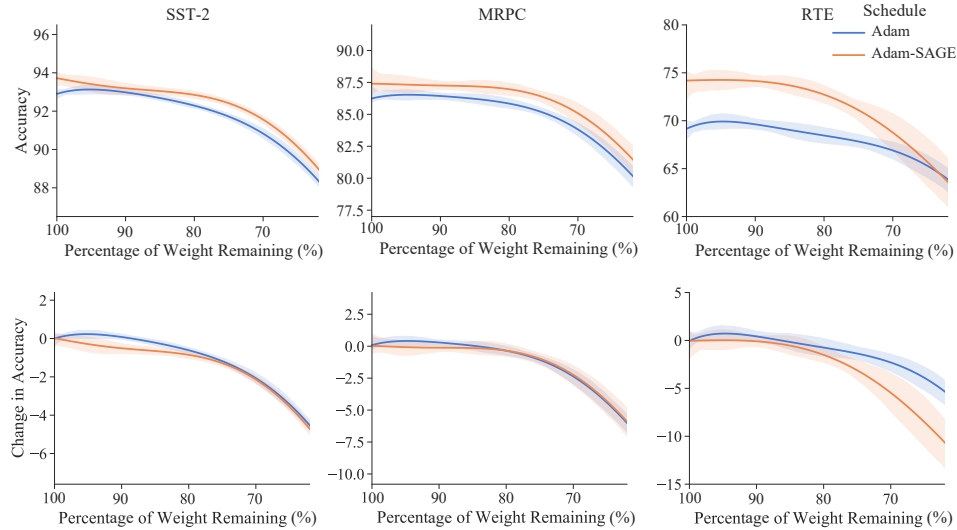


Figure 3: *Upper*: Model generalization performance at different pruning ratios; *Lower*: Change in generalization performance with respect to the full model. Pruning is conducted on the fine-tuned BERT-base models.

We have the following observations:

- The pruning performance of the SAGE optimized models remains higher than that of the baseline models (Figure 3 *Upper*).
- Even the most redundant parameters in the SAGE optimized models makes contributions (Figure 3 *Lower*). When there are over 80% of weights remaining, the pruning performance of the baseline

⁶Embedding weights are excluded.

models is comparable or even superior than their un-pruned alternatives. In contrast, the performance of the SAGE optimized models consistently deteriorates. This suggests that the most redundant parameters in the baseline models fail to contribute, while those in the SAGE optimized models are trained more sufficiently and are able to make contributions.

Sensitivity is a reliable indicator of redundancy. We visualize the local temporal variation (Figure 4) to verify that sensitivity indeed becomes a more reliable indicator of redundancy in SAGE than in the baselines. We track the variation for all parameters in the BERT-base model at each iteration, and we evaluate the variation based on the current mini-batch of training data. See Appendix A.4.2 for implementation details.

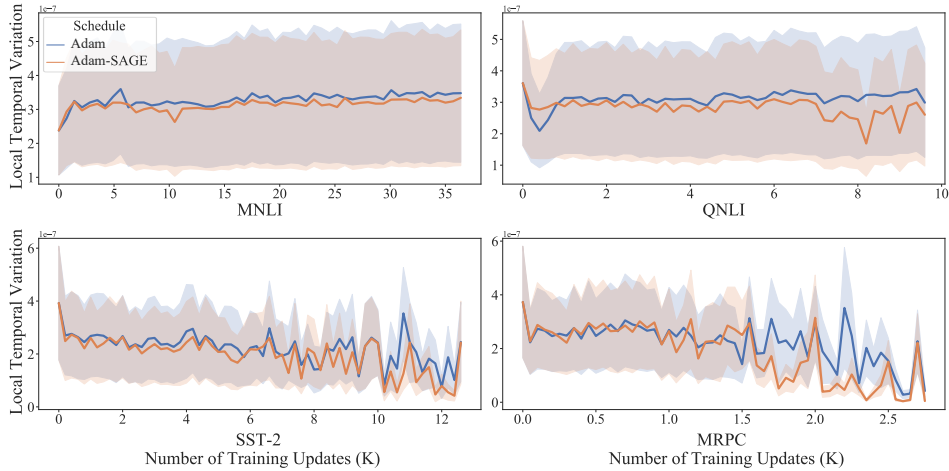


Figure 4: The local temporal variation of sensitivity (with $\beta_0 = 0.7$) during training.

We observe that the local temporal variation in SAGE remains lower or decreases faster than in the baselines for all tasks. For example, the variation in the baseline approach remains large in QNLI. In contrast, the variation in SAGE decreases, suggesting the sensitivity indeed stabilizes and becomes a reliable indicator of redundancy.

5.2 SAGE LEADS TO BETTER GENERALIZATION PERFORMANCE

We verify that SAGE leads to better generalization performance through inspecting the learning curves, decision boundary and hyper-parameter search space.

Learning Curves. Figure 6 shows the training loss, validation loss, learning rate, and sensitivity score obtained by fine-tuning BERT-base on SST-2. All experiment details are deferred to Appendix A.4.3. We have two major observations: 1) SAGE’s validation loss descends faster and SAGE is less prone to overfitting. This observation suggests that SAGE has a regularization effect and reduces the model variance. 2) SAGE’s variance of the sensitivity score becomes lower through training, aligning with our observation in Figure 2. This suggests that SAGE gives rise to a more balanced and sufficient training. Both observations agree with our initial motivation (Figure 1) that redundancy elimination can lead to better generalization.

Hyper-parameter Study. Figure 7 shows the validation accuracy heatmap obtained by fine-tuning BERT-base on the RTE dataset. We plot the accuracy obtained by training with different learning rates, Adam’s β s and SAGE’s β_0 s. We can observe that SAGE consistently achieves a better generalization performance within a larger region of hyper-parameter search space under different β_0 s. We also provide a hyper-parameter study for more datasets in Appendix A.4.5.

Decision Boundary. Figure 5 shows the decision boundary predicted with Adam and SAGE on the Spiral dataset. Specifically, we train a multi-layer perceptron with 3 hidden layers, each with a hidden

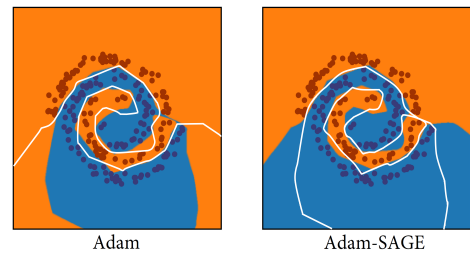


Figure 5: Decision boundary predicted on the Spiral dataset. The white curve on Adam-SAGE corresponds the decision boundary of Adam.

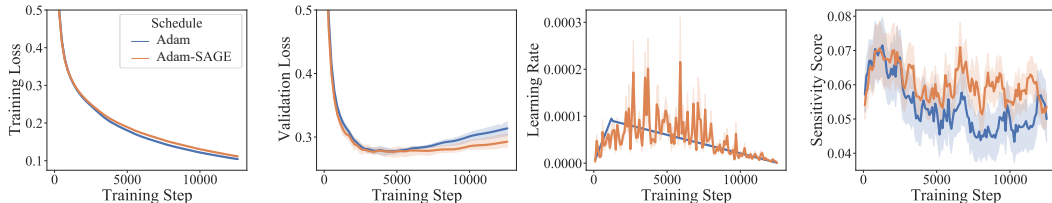


Figure 6: Learning curves obtained by fine-tuning BERT-base on SST-2 dataset.

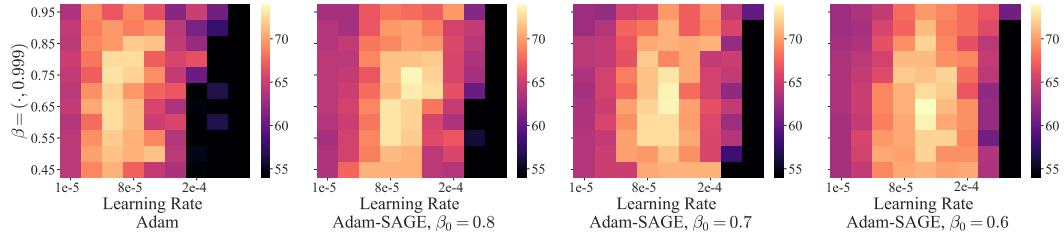


Figure 7: Validation accuracy obtained by fine-tuning BERT-base on RTE dataset with a wide range of hyper-parameters.

dimension of 100. The decision boundary predicted with SAGE is smoother and has a larger margin than with Adam, suggesting SAGE produces a better generalized model.

5.3 COMBINE WITH STATE-OF-THE-ART METHODS

We further show that SAGE is complementary to existing state-of-the-art regularization methods. Specifically, we apply SAGE to SMART (Jiang et al., 2019), a state-of-the-art smoothness-inducing adversarial regularization method. As shown in Table 6, SAGE can further improve upon SMART, suggesting the two techniques are complementary.

Model	Optimizer	RTE Acc	MRPC Acc/F1	CoLA Mcc	SST-2 Acc	STS-B P/S Corr	QNLI Acc	QQP Acc/F1	MNLI-m/mm Acc	Average Score
BERT _{BASE}	Adamax	69.2	86.2/90.4	57.8	92.9	89.7/89.2	91.2	90.9/88.0	84.5/84.4	82.8
SMART _{BASE}	Adamax	72.5	87.7/91.4	59.5	93.5	90.0/89.6	91.9	91.7/88.9	85.2/85.7	84.1
	Adamax-SAGE	75.1	89.0/92.8	60.8	94.3	90.1/89.7	92.2	91.9/89.1	85.9/86.0	85.0

Table 6: Single task fine-tuning dev results on GLUE.

6 DISCUSSION

SAGE is complementary to Adaptive Gradient Methods. Our proposed method and the mainstream adaptive gradient methods (e.g., Adam and AdaGrad) are for fundamentally different purposes. The mainstream adaptive gradient methods aim to improve optimization by adapting to the optimization landscape, while SAGE aims to improve generalization by eliminating the weight redundancy. The quantities of our interest (i.e., Eq. (2) and Eq. (3)) are related to the weight redundancy. They are not directly related to the moduli of the objective function, e.g., smoothness, curvature (which are of the interests for optimization). As shown in our experiments (See Section 4), we do not observe any conflicts between the two methods, as SAGE improves the model generalization performance when being combined with several adaptive gradient methods (e.g., Adam).

Redundant Weights vs. Insufficiently Trained Weights. Lottery Ticket Hypothesis (Frankle & Carbin, 2018) suggests that, in a randomly initialized network, there exists a well-initialized subnetwork, which outperforms any other subnetworks and matches the full model’s performance. This suggests the rest parameters contribute marginally to the model performance. Although the initialization of these parameters may not be satisfactory, SAGE provides them sufficient training so that they can learn to contribute.

7 CONCLUSION

We begin with a hypothesis that the redundant parameters can become useful if they are sufficiently trained by desirable optimization strategies. We verify this hypothesis by proposing an adaptive learning schedule – SAGE, which excites the under-fitted parameters to reduce redundancy and regularize the well-fitted parameters to prevent overfitting. We demonstrate that SAGE can benefit model generalization in a wide range of tasks and strengthen various types of optimizers.

REFERENCES

Roy Bar-Haim, Ido Dagan, Bill Dolan, Lisa Ferro, and Danilo Giampiccolo. The second PASCAL recognising textual entailment challenge. In *Proceedings of the Second PASCAL Challenges Workshop on Recognising Textual Entailment*, 01 2006.

Brian R Bartoldson, Ari S Morcos, Adrian Barbu, and Gordon Erlebacher. The generalization-stability tradeoff in neural network pruning. *arXiv preprint arXiv:1906.03728*, 2019.

Luisa Bentivogli, Ido Dagan, Hoa Trang Dang, Danilo Giampiccolo, and Bernardo Magnini. The fifth pascal recognizing textual entailment challenge. In *In Proc Text Analysis Conference (TAC'09)*, 2009.

Ondřej Bojar, Rajen Chatterjee, Christian Federmann, Yvette Graham, Barry Haddow, Matthias Huck, Antonio Jimeno Yepes, Philipp Koehn, Varvara Logacheva, Christof Monz, et al. Findings of the 2016 conference on machine translation. In *Proceedings of the First Conference on Machine Translation: Volume 2, Shared Task Papers*, pp. 131–198, 2016.

Tom B Brown, Benjamin Mann, Nick Ryder, Melanie Subbiah, Jared Kaplan, Prafulla Dhariwal, Arvind Neelakantan, Pranav Shyam, Girish Sastry, Amanda Askell, et al. Language models are few-shot learners. *arXiv preprint arXiv:2005.14165*, 2020.

Daniel Cer, Mona Diab, Eneko Agirre, Iñigo Lopez-Gazpio, and Lucia Specia. Semeval-2017 task 1: Semantic textual similarity multilingual and crosslingual focused evaluation. In *Proceedings of the 11th International Workshop on Semantic Evaluation (SemEval-2017)*, pp. 1–14, 2017.

Mauro Cettolo, Jan Niehues, Sebastian Stüker, Luisa Bentivogli, Roldano Cattoni, and Marcello Federico. The iwslt 2015 evaluation campaign. In *IWSLT 2015, International Workshop on Spoken Language Translation*, 2015.

Tianlong Chen, Jonathan Frankle, Shiyu Chang, Sijia Liu, Yang Zhang, Zhangyang Wang, and Michael Carbin. The lottery ticket hypothesis for pre-trained bert networks. *arXiv preprint arXiv:2007.12223*, 2020.

Ido Dagan, Oren Glickman, and Bernardo Magnini. The pascal recognising textual entailment challenge. In *Proceedings of the First International Conference on Machine Learning Challenges: Evaluating Predictive Uncertainty Visual Object Classification, and Recognizing Textual Entailment, MLCW'05*, pp. 177–190, Berlin, Heidelberg, 2006. Springer-Verlag. ISBN 3-540-33427-0, 978-3-540-33427-9. doi: 10.1007/11736790_9. URL http://dx.doi.org/10.1007/11736790_9.

Jia Deng, Wei Dong, Richard Socher, Li-Jia Li, Kai Li, and Li Fei-Fei. Imagenet: A large-scale hierarchical image database. In *2009 IEEE conference on computer vision and pattern recognition*, pp. 248–255. Ieee, 2009.

Jacob Devlin, Ming-Wei Chang, Kenton Lee, and Kristina Toutanova. Bert: Pre-training of deep bidirectional transformers for language understanding. *arXiv preprint arXiv:1810.04805*, 2018.

Xiaohan Ding, Guiguang Ding, Xiangxin Zhou, Yuchen Guo, Jungong Han, and Ji Liu. Global sparse momentum sgd for pruning very deep neural networks. *arXiv preprint arXiv:1909.12778*, 2019.

William B Dolan and Chris Brockett. Automatically constructing a corpus of sentential paraphrases. In *Proceedings of the Third International Workshop on Paraphrasing (IWP2005)*, 2005.

Alexey Dosovitskiy, Lucas Beyer, Alexander Kolesnikov, Dirk Weissenborn, Xiaohua Zhai, Thomas Unterthiner, Mostafa Dehghani, Matthias Minderer, Georg Heigold, Sylvain Gelly, et al. An image is worth 16x16 words: Transformers for image recognition at scale. *arXiv preprint arXiv:2010.11929*, 2020.

John Duchi, Elad Hazan, and Yoram Singer. Adaptive subgradient methods for online learning and stochastic optimization. *Journal of machine learning research*, 12(7), 2011.

Angela Fan, Edouard Grave, and Armand Joulin. Reducing transformer depth on demand with structured dropout. *arXiv preprint arXiv:1909.11556*, 2019.

Pierre Foret, Ariel Kleiner, Hossein Mobahi, and Behnam Neyshabur. Sharpness-aware minimization for efficiently improving generalization. *arXiv preprint arXiv:2010.01412*, 2020.

Jonathan Frankle and Michael Carbin. The lottery ticket hypothesis: Finding sparse, trainable neural networks. *arXiv preprint arXiv:1803.03635*, 2018.

Danilo Giampiccolo, Bernardo Magnini, Ido Dagan, and Bill Dolan. The third PASCAL recognizing textual entailment challenge. In *Proceedings of the ACL-PASCAL Workshop on Textual Entailment and Paraphrasing*, pp. 1–9, Prague, June 2007. Association for Computational Linguistics. URL <https://www.aclweb.org/anthology/W07-1401>.

Peter D Grünwald and Abhijit Grunwald. *The minimum description length principle*. 2007.

Pengcheng He, Xiaodong Liu, Jianfeng Gao, and Weizhu Chen. Deberta: Decoding-enhanced bert with disentangled attention. *arXiv preprint arXiv:2006.03654*, 2020.

Geoffrey Hinton, Nitish Srivastava, and Kevin Swersky. Neural networks for machine learning lecture 6a overview of mini-batch gradient descent. *Cited on*, 14(8), 2012.

Lu Hou, Zhiqi Huang, Lifeng Shang, Xin Jiang, Xiao Chen, and Qun Liu. Dynabert: Dynamic bert with adaptive width and depth. *arXiv preprint arXiv:2004.04037*, 2020.

Haoming Jiang, Pengcheng He, Weizhu Chen, Xiaodong Liu, Jianfeng Gao, and Tuo Zhao. Smart: Robust and efficient fine-tuning for pre-trained natural language models through principled regularized optimization. *arXiv preprint arXiv:1911.03437*, 2019.

Diederik P Kingma and Jimmy Ba. Adam: A method for stochastic optimization. *arXiv preprint arXiv:1412.6980*, 2014.

Alex Krizhevsky, Geoffrey Hinton, et al. Learning multiple layers of features from tiny images. 2009.

Yann LeCun, John S Denker, and Sara A Solla. Optimal brain damage. In *Advances in neural information processing systems*, pp. 598–605, 1990.

Namhoon Lee, Thalaiyasingam Ajanthan, and Philip HS Torr. Snip: Single-shot network pruning based on connection sensitivity. *arXiv preprint arXiv:1810.02340*, 2018.

Chen Liang, Simiao Zuo, Minshuo Chen, Haoming Jiang, Xiaodong Liu, Pengcheng He, Tuo Zhao, and Weizhu Chen. Super tickets in pre-trained language models: From model compression to improving generalization. *arXiv preprint arXiv:2105.12002*, 2021.

Liyuan Liu, Haoming Jiang, Pengcheng He, Weizhu Chen, Xiaodong Liu, Jianfeng Gao, and Jiawei Han. On the variance of the adaptive learning rate and beyond. *arXiv preprint arXiv:1908.03265*, 2019a.

Xiaodong Liu, Yu Wang, Jianshu Ji, Hao Cheng, Xueyun Zhu, Emmanuel Awa, Pengcheng He, Weizhu Chen, Hoifung Poon, Guihong Cao, et al. The microsoft toolkit of multi-task deep neural networks for natural language understanding. In *Proceedings of the 58th Annual Meeting of the Association for Computational Linguistics: System Demonstrations*, pp. 118–126, 2020.

Yinhan Liu, Myle Ott, Naman Goyal, Jingfei Du, Mandar Joshi, Danqi Chen, Omer Levy, Mike Lewis, Luke Zettlemoyer, and Veselin Stoyanov. Roberta: A robustly optimized bert pretraining approach. *arXiv preprint arXiv:1907.11692*, 2019b.

Zhuang Liu, Mingjie Sun, Tinghui Zhou, Gao Huang, and Trevor Darrell. Rethinking the value of network pruning. *arXiv preprint arXiv:1810.05270*, 2018.

Ilya Loshchilov and Frank Hutter. Fixing weight decay regularization in adam. 2018.

Ekdeep Singh Lubana and Robert P Dick. A gradient flow framework for analyzing network pruning. *arXiv preprint arXiv:2009.11839*, 2020.

Paul Michel, Omer Levy, and Graham Neubig. Are sixteen heads really better than one? *arXiv preprint arXiv:1905.10650*, 2019.

Pavlo Molchanov, Stephen Tyree, Tero Karras, Timo Aila, and Jan Kautz. Pruning convolutional neural networks for resource efficient inference. *arXiv preprint arXiv:1611.06440*, 2016.

Pavlo Molchanov, Arun Mallya, Stephen Tyree, Iuri Frosio, and Jan Kautz. Importance estimation for neural network pruning. In *Proceedings of the IEEE/CVF Conference on Computer Vision and Pattern Recognition*, pp. 11264–11272, 2019.

Ari S Morcos, Haonan Yu, Michela Paganini, and Yuandong Tian. One ticket to win them all: generalizing lottery ticket initializations across datasets and optimizers. *arXiv preprint arXiv:1906.02773*, 2019.

Michael C Mozer and Paul Smolensky. Skeletonization: A technique for trimming the fat from a network via relevance assessment. In *Advances in neural information processing systems*, pp. 107–115, 1989.

Myle Ott, Sergey Edunov, David Grangier, and Michael Auli. Scaling neural machine translation. *arXiv preprint arXiv:1806.00187*, 2018.

Myle Ott, Sergey Edunov, Alexei Baevski, Angela Fan, Sam Gross, Nathan Ng, David Grangier, and Michael Auli. fairseq: A fast, extensible toolkit for sequence modeling. In *Proceedings of NAACL-HLT 2019: Demonstrations*, 2019.

Pranav Rajpurkar, Jian Zhang, Konstantin Lopyrev, and Percy Liang. SQuAD: 100,000+ questions for machine comprehension of text. In *Proceedings of the 2016 Conference on Empirical Methods in Natural Language Processing*, pp. 2383–2392, Austin, Texas, November 2016. Association for Computational Linguistics. doi: 10.18653/v1/D16-1264. URL <https://www.aclweb.org/anthology/D16-1264>.

Carl Edward Rasmussen and Zoubin Ghahramani. Occam’s razor. *Advances in neural information processing systems*, pp. 294–300, 2001.

Herbert Robbins and Sutton Monro. A stochastic approximation method. *The annals of mathematical statistics*, pp. 400–407, 1951.

Victor Sanh, Thomas Wolf, and Alexander M Rush. Movement pruning: Adaptive sparsity by fine-tuning. *arXiv preprint arXiv:2005.07683*, 2020.

Rico Sennrich, Barry Haddow, and Alexandra Birch. Edinburgh neural machine translation systems for wmt 16. *arXiv preprint arXiv:1606.02891*, 2016.

Richard Socher, Alex Perelygin, Jean Wu, Jason Chuang, Christopher D Manning, Andrew Ng, and Christopher Potts. Recursive deep models for semantic compositionality over a sentiment treebank. In *Proceedings of the 2013 conference on empirical methods in natural language processing*, pp. 1631–1642, 2013.

Lucas Theis, Iryna Korshunova, Alykhan Tejani, and Ferenc Huszár. Faster gaze prediction with dense networks and fisher pruning. *arXiv preprint arXiv:1801.05787*, 2018.

Ashish Vaswani, Noam Shazeer, Niki Parmar, Jakob Uszkoreit, Llion Jones, Aidan N Gomez, Łukasz Kaiser, and Illia Polosukhin. Attention is all you need. *arXiv preprint arXiv:1706.03762*, 2017.

Elena Voita, David Talbot, Fedor Moiseev, Rico Sennrich, and Ivan Titov. Analyzing multi-head self-attention: Specialized heads do the heavy lifting, the rest can be pruned. *arXiv preprint arXiv:1905.09418*, 2019.

Alex Wang, Amanpreet Singh, Julian Michael, Felix Hill, Omer Levy, and Samuel R Bowman. Glue: A multi-task benchmark and analysis platform for natural language understanding. *arXiv preprint arXiv:1804.07461*, 2018.

Ziheng Wang, Jeremy Wohlwend, and Tao Lei. Structured pruning of large language models. *arXiv preprint arXiv:1910.04732*, 2019.

Alex Warstadt, Amanpreet Singh, and Samuel R Bowman. Neural network acceptability judgments. *Transactions of the Association for Computational Linguistics*, 7:625–641, 2019.

Adina Williams, Nikita Nangia, and Samuel Bowman. A broad-coverage challenge corpus for sentence understanding through inference. In *Proceedings of the 2018 Conference of the North American Chapter of the Association for Computational Linguistics: Human Language Technologies, Volume 1 (Long Papers)*, pp. 1112–1122. Association for Computational Linguistics, 2018. URL <http://aclweb.org/anthology/N18-1101>.

Xia Xiao, Zigeng Wang, and Sanguthevar Rajasekaran. Autoprune: Automatic network pruning by regularizing auxiliary parameters. *Advances in neural information processing systems*, 32, 2019.

Matthew D Zeiler. Adadelta: an adaptive learning rate method. *arXiv preprint arXiv:1212.5701*, 2012.

A APPENDIX

A.1 NATURAL LANGUAGE UNDERSTANDING

A.1.1 DATA

GLUE is a collection of nine NLU tasks. The benchmark includes question answering (Rajpurkar et al., 2016), linguistic acceptability (CoLA, Warstadt et al. 2019), sentiment analysis (SST, Socher et al. 2013), text similarity (STS-B, Cer et al. 2017), paraphrase detection (MRPC, Dolan & Brockett 2005), and natural language inference (RTE & MNLI, Dagan et al. 2006; Bar-Haim et al. 2006; Giampiccolo et al. 2007; Bentivogli et al. 2009; Williams et al. 2018) tasks. Details of the GLUE benchmark, including tasks, statistics, and evaluation metrics, are summarized in Table 13.

All the texts were tokenized using wordpieces, and were chopped to spans no longer than 512 tokens.

A.1.2 TRAINING DETAILS

To fine-tune BERT-base and RoBERTa-large models on individual tasks, we append a task-specific fully-connected classification layer to them as in Devlin et al. (2018).

Table 7 present the hyper-parameter configurations. We tune this set of hyper-parameters on a single seed, and report the averaged results obtained with the same configuration over all seeds. For SAGE experiments, We slightly tune β_0 within a range of 0.1 on different seeds. We apply a linear weight decay rate of 0.01 and a gradient norm clipping threshold of 1 for all experiments. All experiments are conducted on Nvidia V100 GPUs.

Hyper-param	Experiment	RTE	MRPC	CoLA	SST-2	STS-B	QNLI	QQP	MNLI
Learning Rate	BERT _{BASE} , Adam	1e-5	1e-5	1e-5	1e-5	1e-5	1e-5	2e-5	2e-5
	BERT _{BASE} , Adam-SAGE	1e-4	8e-5	8e-5	3e-5	1e-4	8e-5	4e-5	5e-5
	BERT _{BASE} , Adamax	1e-4	1e-4	1e-4	5e-5	1e-4	1e-4	1e-4	8e-5
	BERT _{BASE} , Adamax-SAGE	3e-4	3e-4	2e-4	2e-4	5e-4	5e-4	3e-4	2e-4
	RoBERTa _{LARGE} , Adamax	5e-5	5e-5	3e-5	1e-5	5e-5	1e-5	1e-4	1e-5
	RoBERTa _{LARGE} , Adamax-SAGE	6e-5	2e-4	8e-5	2e-5	8e-5	3e-5	2e-4	8e-5
β_0	BERT _{BASE} , Adam-SAGE	0.60	0.80	0.70	0.80	0.60	0.70	0.75	0.70
	BERT _{BASE} , Adamax-SAGE	0.65	0.80	0.75	0.70	0.75	0.70	0.75	0.85
	RoBERTa _{LARGE} , Adamax-SAGE	0.75	0.65	0.70	0.75	0.80	0.80	0.65	0.60
Batch Size	BERT _{BASE}	16	8	32	32	32	32	32	32
	RoBERTa _{LARGE}	16	8	32	32	32	32	32	32
Epoch	BERT _{BASE}	6	6	6	6	6	3	6	3
	RoBERTa _{LARGE}	15	6	6	6	10	10	15	3
Dropout	BERT _{BASE}	0.1	0.1	0.1	0.1	0.1	0.1	0.0	0.3
	RoBERTa _{LARGE}	0.1	0.1	0.1	0.1	0.1	0.1	0.0	0.3
Warmup	BERT _{BASE}	0.1	0.1	0.1	0.1	0.1	0.1	0.0	0.1
	RoBERTa _{LARGE}	0.1	0.1	0.1	0.1	0.1	0.1	0.1	0.1

Table 7: Hyper-parameter configurations for GLUE experiments. “Epoch” refers to the total training epochs; we adopt early-stopping strategy in practice. “Dropout” refers to classification layer dropout ratio. “Warmup” refers to the ratio of learning rate linear warmup iterations to total training iterations.

A.1.3 EVALUATION RESULTS

Statistics of the dev set results. Table 8 shows the standard deviation of the dev set results.

Average score computation formula. For dev set results, we first obtain a score for each task by averaging the scores of all metrics (e.g., Acc and F1) and test sets (e.g., MNLI-m and MNLI-mm) within this task, then compute a task-average score. For test set results, we directly averages scores of all reported metrics following Devlin et al. (2018).

Model	Optimizer	RTE	MRPC	CoLA	SST-2	STS-B	QNLI	QQP	MNLI
BERT _{BASE}	Adam-SAGE	0.35	0.32	0.85	0.25	0.12	0.06	0.05	0.06
	Adamax-SAGE	0.56	0.69	0.12	0.23	0.03	0.06	0.08	0.10
RoBERTa _{LARGE}	Adamax-SAGE	0.51	0.78	0.50	0.19	0.08	0.00	0.05	0.05

Table 8: Standard deviation of the dev set results.

A.2 NEURAL MACHINE TRANSLATION

A.2.1 DATA

Table 9 shows the number of sentence pairs in each dataset. We use the standard newstest-2013 and newstest-2014 as dev and test set for WMT’16 En-De. We follow Ott et al. (2019) to split the dev/test sets for IWSLT’14 De-En.

All datasets are encoded using byte-pair encoding (BPE, Sennrich et al. (2016)). We preprocess IWSLT’14 De-En data following *fairseq*⁷ and adopt the preprocessed WMT’16 En-De from Google⁸.

Data	Train	Dev	Test
IWSLT’14 De-En	160K	7283	6750
WMT’16 En-De	4.5M	1061	1019

Table 9: The number of parallel sentences in NMT datasets.

A.2.2 TRAINING DETAILS

We adopt the Transformer-base model for both datasets. For IWSLT’14 De-En, we share the decoder and encoder output embeddings. For WMT’16 En-De, we share all the embeddings.

Table 10 presents the hyper-parameter configurations for the best models. We apply a linear weight decay rate of 1×10^{-4} and a label smoothing ratio of 0.1 for all experiments. All experiments are conducted on Nvidia V100 GPUs.

For IWSLT’14 De-En, we report the BLEU score of the best checkpoint using a beam size of 5 and length penalty of 1. For WMT’16 En-De, we report the average of the last 10 checkpoints with a beam size of 4 and length penalty of 0.6.

Hyper-param	Experiment	IWSLT’14 De-En	WMT’16 En-De
Learning Rate	Adam	5e-4	7e-4
	Adam-SAGE	1e-3	2e-3
β_0	Adam-SAGE	0.8	0.4
Batch size	Both	4096	32768
Epoch	Both	60	40
Dropout	Both	0.3	0.1
Warmup	Both	8000	4000

Table 10: Hyper-parameter configurations for NMT experiments. “Warmup” refers to the learning rate linear warmup iterations.

⁷<https://github.com/pytorch/fairseq/blob/master/examples/translation>

⁸https://pytorchnlp.readthedocs.io/en/latest/_modules/torchnlp/datasets/wmt.html

A.3 IMAGE CLASSIFICATION

A.3.1 DATA

For CIFAR100, we apply random cropping and random horizontal flipping to the training data.

A.3.2 TRAINING DETAILS

Table 11 present the hyper-parameter configurations for the best models. All experiments are conducted on Nvidia V100 GPUs.

Hyper-param	Experiment	CIFAR100	ImageNet
Learning Rate	ViT-B/32, SGD-SAGE	0.02	0.05
	ViT-L/32, SGD-SAGE	0.02	0.08
β_0	ViT-B/32, SGD-SAGE	0.95	0.95
	ViT-L/32, SGD-SAGE	0.85	0.95
Training Steps	All	10000	20000
Dropout	All	0.0	0.0

Table 11: Hyper-parameter configurations for ViT experiments on CIFAR100 and ImageNet.

A.4 SUPPLEMENTS FOR METHOD AND ANALYSIS

A.4.1 ADAM-SAGE ALGORITHM

Algorithm 2 Adam-SAGE (\odot denotes Hadamard product and \oslash denotes Hadamard division)

Input: Model parameters $\Theta \in \mathbb{R}^J$; Data \mathcal{D} ; Learning rate schedule $\eta(\cdot)$; Total training iteration T ; Moving average coefficient $\beta_0, \beta_1, \beta_2$.

- 1: Initialize $\widehat{I}^{(0)}, m^{(0)}, v^{(0)} = \mathbf{0} \in \mathbb{R}^J$.
- 2: **for** $t = 1, \dots, T$ **do**
- 3: Sample a minibatch $b^{(t)}$ from \mathcal{D} .
- 4: Compute gradient $g^{(t)} = \nabla_{\Theta^{(t)}} L(b^{(t)}, \Theta^{(t)})$.
- 5: Compute sensitivity $I^{(t)} = |\Theta^{(t)} \odot g^{(t)}|$.
- 6: $m^{(t)} = \beta_1 m^{(t-1)} + (1 - \beta_1) g^{(t)}$
- 7: $v^{(t)} = \beta_2 v^{(t-1)} + (1 - \beta_2) (g^{(t)})^2$
- 8: $\widehat{I}^{(t)} = \beta_0 \widehat{I}^{(t-1)} + (1 - \beta_0) I^{(t)}$.
- 9: $\widehat{m}^{(t)} = m^{(t)} / (1 - \beta_1)$
- 10: $\widehat{v}^{(t)} = v^{(t)} / (1 - \beta_2)$
- 11: $\widehat{I}^{(t)} = \widehat{I}^{(t)} / (1 - \beta_0)$
- 12: $U^{(t)} = |I^{(t)} - \widehat{I}^{(t)}|$.
- 13: Update $\Theta^{(t+1)} = \Theta^{(t)} - \eta^{(t)} ((U^{(t)} + \epsilon) \odot \widehat{m}^{(t)}) \oslash ((\widehat{I}^{(t)} + \epsilon) \odot (\sqrt{\widehat{v}^{(t)}} + \epsilon)) \odot g^{(t)}$.
- 14: **end for**

A.4.2 IMPLEMENTATION DETAILS FOR SECTION 5.1

Figure 2 experiments: Due to the extremely large model size, we only sample 110K parameters per layer (in total $12 \times 110K$ parameters) to calculate the distribution. We select the hyper-parameters that yield the best generalization performance on the BERT-base model, and we evaluate the sensitivity of each parameter using the entire training set.

Figure 4 experiments: Following previous experiment’s practice, we randomly sample 110K parameters per layer (in total $12 \times 110K$ parameters), and for visualization purposes, we plot 60 randomly selected iterations. We adopt the learning rate corresponding to the best training performance for both SAGE and the baselines.

A.4.3 IMPLEMENTATION DETAILS FOR SECTION 5.2

Plotting the parameter sensitivity distribution throughout training can be computational expensive. The distribution varies significantly throughout training and often fails to provide a meaningful visualisation. As a result, we compute the structured sensitivity score instead of the parameter sensitivity score. Specifically, we compute a single sensitivity score for each Transformer weight block Θ at iteration t using the structured counterpart of the parameter sensitivity metric widely adopted in the existing structured pruning literature (Michel et al., 2019; Liang et al., 2021). Following common structured pruning practice, we split Transformer models into 12 feed-forward weight modules and 12 multi-head attention weight modules, and plot the average and variance of the sensitivity of these modules’ sensitivity scores throughout the training.

We present the results obtained with the hyper-parameters that yield the best generalization performance on the BERT-base model for both Adamax (Baseline) and Adamax-SAGE (SAGE).

A.4.4 ABLATION STUDY

To further interpret the role of the parameter sensitivity I and the local temporal variation U , we conduct an ablation study on these two factors. Specifically, we check five variants of Eq. (4):

$$\begin{aligned} \text{Variant 1. } \eta_j^{(t)} &= \eta^{(t)}(\tilde{I}_j^{(t)} + \epsilon)(U_j^{(t)} + \epsilon) \\ \text{Variant 2. } \eta_j^{(t)} &= \eta^{(t)}(\tilde{I}_j^{(t)} + \epsilon)/(U_j^{(t)} + \epsilon) \\ \text{Variant 3. } \eta_j^{(t)} &= \eta^{(t)}(\tilde{I}_j^{(t)} + \epsilon) \\ \text{Variant 4. } \eta_j^{(t)} &= \eta^{(t)}/(\tilde{I}_j^{(t)} + \epsilon) \\ \text{Variant 5. } \eta_j^{(t)} &= \eta^{(t)}(U_j^{(t)} + \epsilon) \end{aligned}$$

For Variants 1,2 and 3, we aim to check the performance of giving a high/low-sensitive parameter a high/low, instead of low/high learning rate. Specifically, we place $(\tilde{I}_j^{(t)} + \epsilon)$ in the numerator, so that the learning rates increase for the high sensitive parameters and decrease for low sensitive parameters.

For Variants 4 and 5, we aim to check the performance of eliminating the influence of one of these factors. Specifically, we fix the local temporal variation term to 1 in Variant 4 and fix the sensitivity term to 1 in Variant 5.

A.4.5 HYPER-PARAMETER STUDY

We investigate the influence of hyper-parameters learning rate and β_0 on the performance of SAGE (Figure 8). As can be seen, SAGE requires a larger learning rate than the baselines to offset the small scale of the modulation term (the optimal baseline learning rate lies in $5 \times 10^{-5} \sim 1 \times 10^{-4}$ for MNLI, $5 \times 10^{-4} \sim 7 \times 10^{-4}$ for IWSLT 14 De-En and $0.1 \sim 0.2$ for CIFAR10). Furthermore, switching to a larger learning rate requires a lower β_0 to maintain the same level of performance.

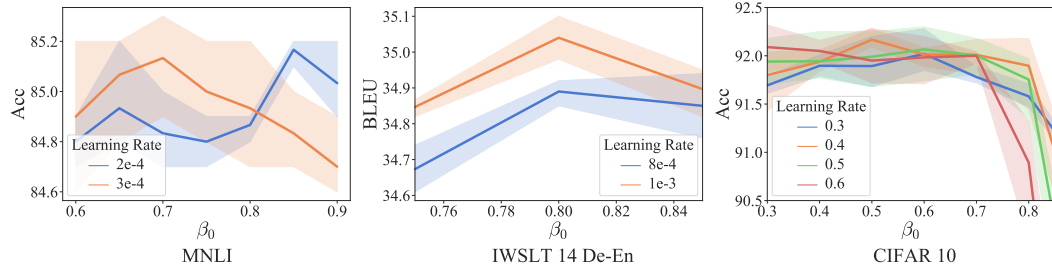


Figure 8: Parameter study on learning rate and β_0 .

All five variants show no clear gain upon the baseline on both RTE and SST-2 datasets after careful hyper-parameter tuning. Specifically, we observe that the Variants 1 and 3 converge very fast at the early stage of training, and then quickly start overfitting. In Variants 2 and 4, the training collapses due to gradient explosion or vanishing.

Variant Name	Learning Rate Modulating Term	RTE	SST-2
Adam	1	63.5	92.9
Adam-SAGE	$(U_j^{(t)} + \epsilon) / (\hat{I}_j^{(t)} + \epsilon)$	73.3	93.5
Variant 1.	$(\hat{I}_j^{(t)} + \epsilon)(U_j^{(t)} + \epsilon)$	63.5	91.2
Variant 2.	$(\hat{I}_j^{(t)} + \epsilon) / (U_j^{(t)} + \epsilon)$	Unconverged	Unconverged
Variant 3.	$\hat{I}_j^{(t)} + \epsilon$	63.8	91.1
Variant 4.	$1 / (\hat{I}_j^{(t)} + \epsilon)$	Unconverged	Unconverged
Variant 5.	$U_j^{(t)} + \epsilon$	63.8	91.1

Table 12: Ablation study on parameter sensitivity and local temporal variations.

Corpus	Task	#Train	#Dev	#Test	#Label	Metrics
Single-Sentence Classification (GLUE)						
CoLA	Acceptability	8.5k	1k	1k	2	Matthews corr
SST	Sentiment	67k	872	1.8k	2	Accuracy
Pairwise Text Classification (GLUE)						
MNLI	NLI	393k	20k	20k	3	Accuracy
RTE	NLI	2.5k	276	3k	2	Accuracy
QQP	Paraphrase	364k	40k	391k	2	Accuracy/F1
MRPC	Paraphrase	3.7k	408	1.7k	2	Accuracy/F1
QNLI	QA/NLI	108k	5.7k	5.7k	2	Accuracy
Text Similarity (GLUE)						
STS-B	Similarity	7k	1.5k	1.4k	1	Pearson/Spearman corr

Table 13: Summary of the GLUE benchmark.